Int. J. Simul. Multidisci. Des. Optim. **12**, 21 (2021)
© A.C. Kuriakose et al., Published by EDP Sciences, 2021
https://doi.org/10.1051/smdo/2021018

IJSMDO
Available online at:
https://www.ijsmdo.org

Computation Challenges for engineering problems

RESEARCH ARTICLE OPEN ACCESS

Experimental investigations and finite element analysis of milling of Inconel 718 alloy

Akhil C. Kuriakose*, Raman Balakrishnan, Harsh Vardhan, and Krishnaraju Srinivasaraju Vijay Sekar

Department of Mechanical Engineering, Sri Sivasubramaniya Nadar College of Engineering, Kalavakkam 603 110, Tamil Nadu, India

Received: 10 January 2021 / Accepted: 10 August 2021

Abstract. Super-alloys encompass great challenges in machinability. One such alloy of much interest in applications is Inconel 718. Its increased hardness, low thermal diffusivity and high temperature strength make it desirable for applications, at the same time rendering its machining a demanding task. Extensive studies have been performed on machinability of Inconel 718, from the turning process stand-point. However, there is found to be a comparative dearth of work on the milling process. Taking into account the versatility of end-milling within the family of milling processes and the research gap, we found that a parametric optimization (aimed at minimum machining forces) of end-milling would be a meaningful effort. An experiment was conducted to study conditions that would help us achieve the same. In our further quest for optimization, chip morphology studies using SEM occupied a special place. Bearing in mind immense prediction capabilities of computer simulations based on FEA available today, we attempted process replication of the experimental work. The significant cutting forces were chosen as the benchmark factor for this purpose and proper attention was given to validation of the FEM created. Such FEM holds promise of being resourceful to drive up efficiency, with consequent spill-over to the production line.

Keywords: Inconel 718 / machinability / process optimization / milling / end-milling / chip morphology / prediction capabilities of FEA / validation of FEM

1 Introduction

Inconel 718 is a Nickel-Chromium-Molybdenum alloy designed to resist a wide range of severely corrosive environments, especially pitting and crevice corrosion. This Nickel-Steel alloy also displays exceptionally high Yield, Tensile, and Creep-Rupture properties at high temperatures. Nickel-base super-alloys like Inconel are generally known to be one of the most difficult- to-machine materials because of their high hardness, strength at elevated temperatures, and low thermal diffusivity. Inconel is also a difficult metal to shape, using traditional cold forming techniques, due to rapid work-hardening. However, in view of extensive applications of such alloys, any attempt at optimizing their machining would be a reward in itself. Today, research work on machining modeling has a focus on predictive ability and is most concentrated in the turning process of metal removal. Important factors of machining such as Cutting Forces, Temperatures, Chip Configuration, Strains and Stresses, if estimated before actual cutting on a machine tool, are seen to cut down unwanted costs to a great extent. Choosing from among the family of milling processes, the versatile end-milling, where there was a comparative lack of research work regarding combined optimization of experimental parameters, we conducted an experiment towards that end and then performed DOE (Design of Experiments) Analysis and ANOVA (Analysis of Variance) on results. As a matter of additional interest, machining chips were subjected to examination with SEM (Scanning Electron Microscopy) for more insights into the cutting process at some selected conditions. Wanting to tap into the modern ability of process simulation of computers, we also embarked on sincere work to simulate the experiment of end-milling by using suitable FEA (Finite Element Analysis) tool. After validation by three methods (comparison with the previous experimental data, performing theoretical parametric extrapolation and chip thickness correlation), the accuracy of FEM (Finite Element Modeling) could be vouched. This model could then be also used for prediction of machining parameters in any range of acceptable regions, which was then undertaken. All results were then put into perspective.

* e-mail: akhil16008@mech.ssn.edu.in

This is an Open Access article distributed under the terms of the Creative Commons Attribution License (https://creativecommons.org/licenses/by/4.0), which permits unrestricted use, distribution, and reproduction in any medium, provided the original work is properly cited.

↓	C1	C2
	Speed	Feed
1	200	20
2	200	50
3	200	80
4	470	20
5	470	50
6	470	80
7	900	20
8	900	50
9	900	80

Fig. 1. L9 array.

Fig. 2. Work-piece.

Fig. 3. Cutting tool.

2 Methods

Following paragraphs explain the 4 adopted methods in sequence: 1. Experiment and DOE 2.Chip Study 3. FEA (Setup and Solution) 4. FEA Validation (Experimental Value Comparison, Material Model Extrapolation and Chip Dimensional Evaluation).

In any machining process, the main parameters are Cutting Speed (or Cutting Velocity), Feed Rate (or Worktable Movement Rate) and Depth of Cut (or Per Machining Pass Depth). However as far as end-milling process is concerned, Depth of Cut as a changing input variable is seen to be not of much significant impact, as evident in literature ideas [1]. So we chose rather to keep it constant at 0.5 mm. Then we are left with Cutting Speed and Feed Rate as impactful input variables. Our output variables were chosen to be Forces of Milling (Cutting Force and Feed Force, both horizontal in orientation, leaving out Thrust Force in vertical direction due to it being negligible in end-milling, at constant depth of cut condition), while our input variables were taken as Cutting Speed (in 'revolutions per minute, rpm', controlled by setting Spindle Speed of the Vertical Milling Machine) and Feed Rate (in 'millimeter per minute, mm/min', controllable by engaging suitable gear combinations in Work-Table Feed arrangement). For the chosen L-9 orthogonal array of machining parameters with three levels (low, medium and high) [2] each in the two input variables (Fig. 1), a suitable size of Inconel 718 plate (Fig. 2) was acquired ($150 \times 80 \times 10$, all in mm) along with a compatible Tungsten Carbide (WC) tool [3,4] of diameter 12 mm (Fig. 3). Then, the experiment (Fig. 4) was performed for chosen conditions and the trends obtained in Machining Forces from Tool-Force Dynamometer (Fig. 5) compared with standard test results [5]. Finally, a statistical study involving DOE Analysis and ANOVA was performed on results obtained by experiment [6], using Minitab, to

investigate the causal relationships that were statistically significant.

Chip morphology is an important aspect in the evaluation of machinability of Inconel 718. Such studies can help determine the nature of machining efficiency at the microstructural level. Along with that, a lot of other insights into material behavior in metal cutting can be obtained with the likes of Chip Reduction Coefficient and features in the cross sectional area of chip [7]. For the present work, the metal chips of Inconel 718 collected after experiments were chosen selectively at specific points of interest in machining parameter ranges to investigate the microstructural level implications [8] of the end-milling process by SEM. For instance, we could observe in various samples of the present work, tubular helix shaped chips with rough surface, segmented chips with abrasive saw-toothed edges, serrations and closely spaced shear bands. All these could give indications of phenomena like shear instability, adiabatic shearing and localization of shear.

After chip morphological studies, FEA was sought to be applied to the end-milling process with a view to simulating using suitable software. Deform 3D appeared an ideal choice due to its obvious capabilities [1]. Adequate attention was given to previous studies and their limitations [9]. In the FEA formulation (Tab. 1), relevant input data like nature of work-tool interaction (friction factor and heat transfer coefficient), dimensional data and element type were carefully entered after proper study [10].

Fig. 4. Vertical milling machine.

Fig. 5. Display unit of tool force dynamometer.

Table 1. FEA formulation.

Item considered for building FEM	Attribute chosen in deform 3D software
Type of Analysis	Lagrangian
Dimensions of FEM	Same as Experiment (No Scaling)
Mesh Size (Aspect) Ratio	2
Element Type	4-noded, 3D Tetrahedral
Number of Elements in Work-piece after Meshing	35171
Number of Nodes in Work-piece after Meshing	7790
Number of Elements in Cutting Tool after Meshing	14651
Number of Nodes in Cutting Tool after Meshing	3526
Nature of Work-piece Deformation	Plastic
Nature of Cutting Tool	Rigid
Relevant Experimental Data	Cutting Speed, Feed Rate & Length of Machining Pass
Contact Modeling	Lagrange Multiplier Method
Material Modeling	Johnson-Cook (JC) Model
Friction Modeling	Usui Model
Friction Factor	0.6
Chip Separation Criteria	Physical Criticality based on JC Model
FEM Renewal	Adaptive Meshing
Heat Transfer Coefficient	45×10^6 W / mm^{2}K
Ambient Temperature	303 K

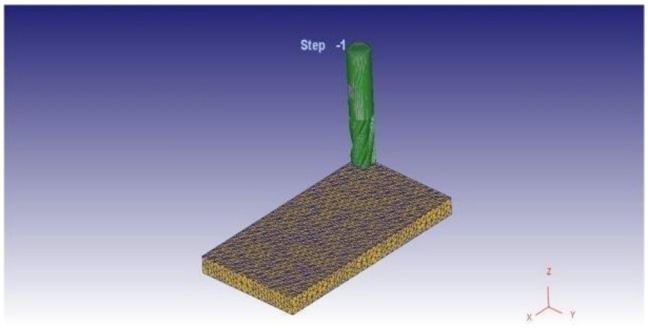

Fig. 6. Combined tool-work system after meshing.

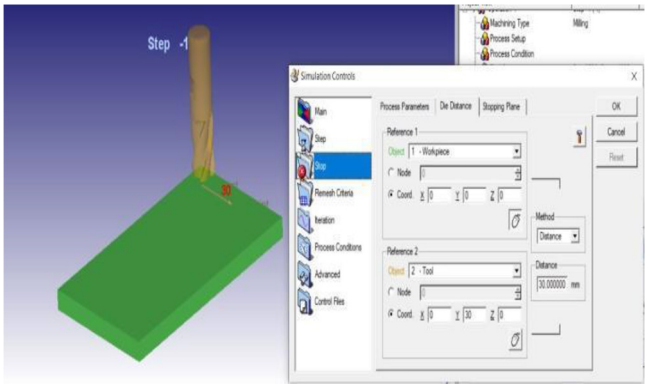

Fig. 7. Process setup (tool travel length).

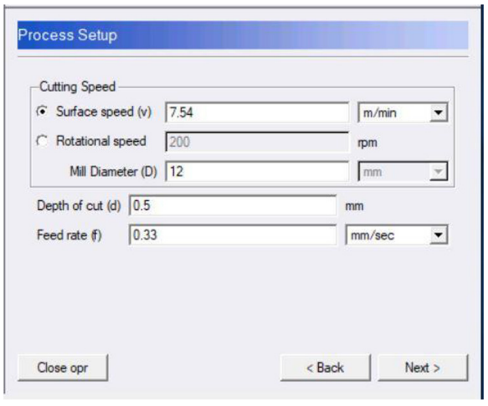

Fig. 8. Process setup (physical boundary conditions).

The Lagrangian analysis along with 4-noded, 3D Tetrahedral Element was used, reposing faith in its advantage to fit to complex arbitrary shaped geometry and consequent control of distortion of elements to a greater extent. The software options (Figs. 6–9) available under boundary conditions (for experimental parameters), material (Johnson-Cook, or JC for short) [4] and friction (Usui) models, contact definition and chip separation criteria were examined before solving our Finite Element Model. After solution, in the post-processing, several relevant output

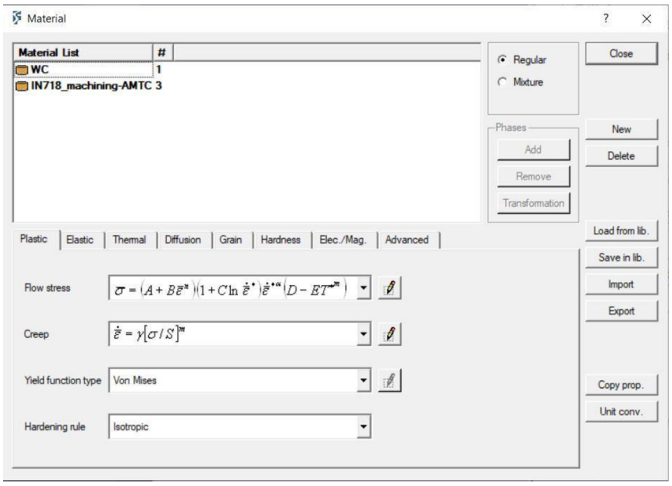

Fig. 9. Process setup (material modeling).

results of FEA, crucial of which included Cutting Force (the main object of interest in this paper), were obtained, including predictive solutions.

After the FEA solution, came the need for validation of FEM utilized. The first apparent choice was direct comparison with experimental force values, which was satisfactory in our case. Another way to validate the model would be to numerically extrapolate the equation of the material model (JC model) and then try to evaluate by comparison, the stability of predictive solutions of FEM. This was done using MS Excel (Fig. 10), with reasonable empirical assumptions of parameters in the JC Model (Tab. 2) for required operating ambient temperature range (by varying 'T'). Remarkable convergence was seen in this step of evaluation too. In addition, another way to vouch for the dimensional correctness of FEM formulated was to match the chip thickness given by the software using 'Ruler' option in the post-processing window (Fig. 11) with actual measurements of corresponding chip samples using a digital micrometer. An index called Chip Dimensional Ratio (CDR), obtained by dividing critical chip dimension by depth of cut, was calculated for both the software values and measured sample values, later to be compared. This again proved satisfactory. Thus, validation of FEM was done in three methods, in all.

Material Flow Stress (MPa) at Ambient Temperature 'T' (K),

$$\sigma = (A + B\varepsilon^n)\left[1 + C\ln\left(\frac{\dot{\varepsilon}}{\dot{\varepsilon}_0}\right)\right]\left[1 - \left(\frac{T - T_r}{T_m - T_r}\right)^m\right]$$

(JC Model equation).

3 Results and discussion

The first set of experimental results is the Force Values (Tab. 3) and their corresponding graphical plots (Figs. 12–17). The standard trend of Cutting Forces against Cutting Speed is one of decreasing nature, owing to

	T(K)	303																			
		0.1	0.2	0.3	0.4	0.5	0.6	0.7	0.8	0.9	1	1.1	1.2	1.3	1.4	1.5	1.6	1.7	1.8	1.9	2
1	10	521.21875	600.519	666.444	724.954	778.502	828.402	875.46	920.213	963.045	1004.24	1044.01	1082.54	1119.96	1156.38	1191.91	1226.61	1260.56	1293.82	1326.44	1358.46
2	100	540.85276	623.14	691.549	752.262	807.828	859.608	908.438	954.877	999.322	1042.07	1083.34	1123.32	1162.15	1199.94	1236.8	1272.81	1308.04	1342.56	1376.4	1409.63
3	1000	560.48676	645.761	716.654	779.571	837.153	890.813	941.416	989.541	1035.6	1079.9	1122.67	1164.1	1204.34	1243.5	1281.7	1319.02	1355.53	1391.29	1426.37	1460.8
4	10000	580.12077	668.382	741.758	806.879	866.479	922.018	974.394	1024.2	1071.88	1117.73	1162	1204.88	1246.52	1287.06	1326.6	1365.22	1403.01	1440.03	1476.34	1511.98
5	100000	599.75478	691.003	766.863	834.188	895.805	953.224	1007.37	1058.87	1108.15	1155.56	1201.32	1245.66	1288.71	1330.62	1371.5	1411.43	1450.5	1488.77	1526.3	1563.15
6	1000000	619.38878	713.625	791.967	861.497	925.131	984.429	1040.35	1093.53	1144.43	1193.38	1240.65	1286.43	1330.9	1374.18	1416.4	1457.64	1497.98	1537.51	1576.27	1614.32

Fig. 10. Snapshot from MS Excel parametric extrapolative values of material flow stress, for ambient temperature $T = 303$ K (For FEM Validation-II).

Table 2. JC model parameters (For FEM Validation-II).

Parameter	Meaning	Typical value/range empirically
A	Reference Yield Stress	368.18 MPa
B	Strain Hardening Constant	600
C	Strengthening Coefficient	0.017
n	Strain Hardening Coefficient	0.65
m	Thermal Softening Coefficient	1.3
ε	Strain	0.1 to 2
$\dot{\varepsilon}$	Strain Rate	10 to 10^6 s^{-1}
$\dot{\varepsilon}_0$	Reference Strain Rate	1 s^{-1}
Tm	Melting Temperature	1570 K
Tr	Transition Temperature	293 K

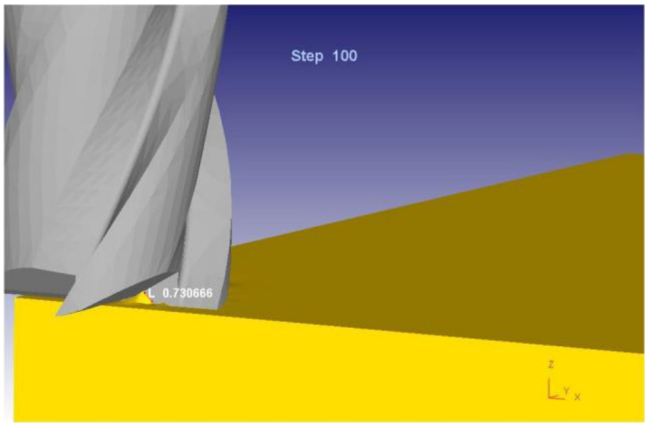

Fig. 11. Critical chip dimension by ruler option from deform 3D Software (For FEM Validation-III).

thermal softening of specimen undergoing cutting [5]. This is by and large true in our case, as can be seen in the plots (Figs. 12–14). The only exception is some midpoints in the Cutting Speed range and the high Feed Rate plot (Fig. 14) where the reverse (increasing) trend is observed for Cutting Force, F_x. This reverse trend is a case of anomalous behavior. Similarly, the standard trend of Cutting Forces against Feed Rate is one of increasing nature, owing to heavier metallic load on the tool [5]. The same is seen in our case (Figs. 15–17), except when venturing into the high Feed Rate regime, where anomaly kicks in. As high Cutting Force (F_x) is detrimental from the standpoint of tool life as well as process stability, we conclude that the regime of high Feed Rates, where such behavior is prone to occur, is not recommendable for Inconel 718 end-milling.

3.1 Graphs of data from experimental results

3.1.1 Results from statistical studies in Minitab

The second set of results involves the twin of statistical studies (DOE Analysis and ANOVA) in Minitab, of which only those with significant implications are being given here (Figs. 18–23). From the Main Effects plots of DOE Analysis (Figs. 18 and 20), it is clear that the dominant parameters of influence for Cutting Force (F_x) and Feed Force (F_y) are Feed Rate and Cutting Speed respectively. This is because the plots show grander spatial inclination (indicating greater magnitude of change) in the mentioned pair regions. From the Interaction plots of DOE Analysis (Figs. 19 and 21), it is observed that inter-parametric influence (interaction between Cutting Speed and Feed rate) is seen to be relatively higher in the case of Feed Force (F_y) than on Cutting Force (F_x). This is due to the fact that in these plots, the lines show greater divergent trends (in terms of comparative slopes) in the graphs corresponding to

Table 3. Experimental results (force values).

Experiment run	Spindle speed (rpm)	Table feed rate (mm/min)	Measured cutting force, F_x (N)	Measured feed force, F_y (N)	Noted machining time (s)
1	200	20	333.54	117.72	124.26
2	470	20	284.49	49.05	124.21
3	900	20	264.87	58.86	123.93
4	200	50	598.41	78.48	51.03
5	470	50	470.88	166.77	50.31
6	900	50	490.5	39.24	50.65
7	200	80	147.15	117.72	30.92
8	470	80	215.82	78.48	31.56
9	900	80	274.68	49.05	31.38

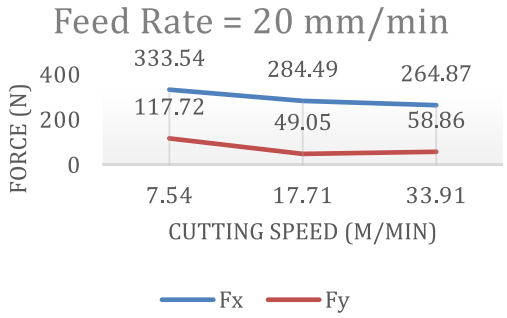

Fig. 12. Forces vs cutting speed at 20 mm/min.

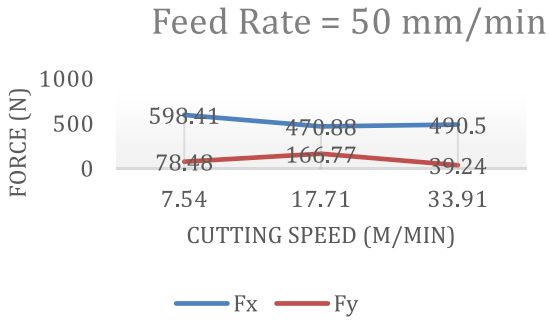

Fig. 13. Forces vs cutting speed at 50 mm/min.

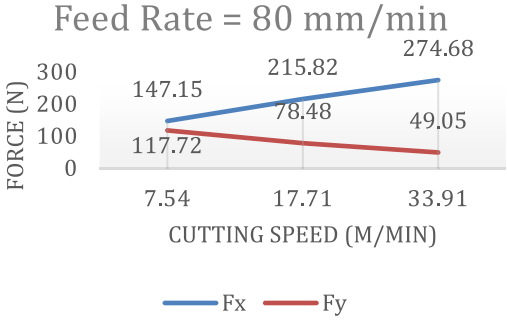

Fig. 14. Forces vs cutting speed at 80 mm/min.

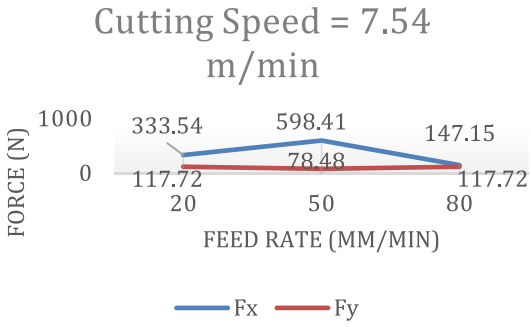

Fig. 15. Forces vs feed rate at 7.54 m/min.

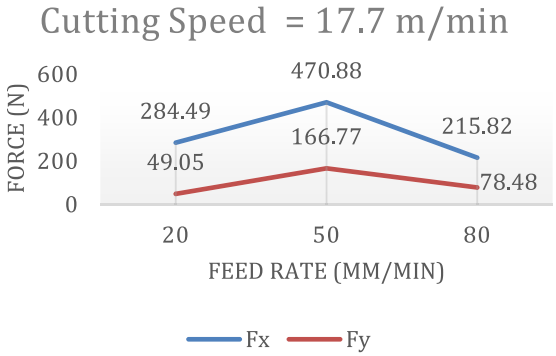

Fig. 16. Forces vs feed rate at 17.7 m/min.

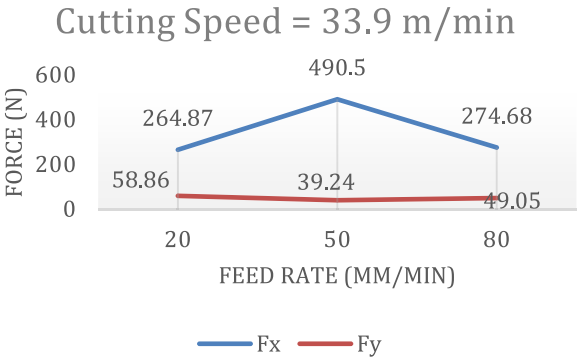

Fig. 17. Forces vs feed rate at 33.9 m/min.

Fig. 18. Main effects plot for cutting force, F_x.

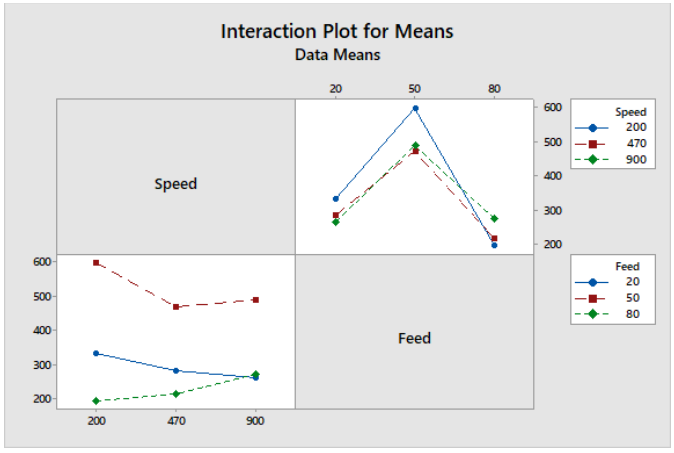

Fig. 19. Interaction plot for Cutting Force, F_x.

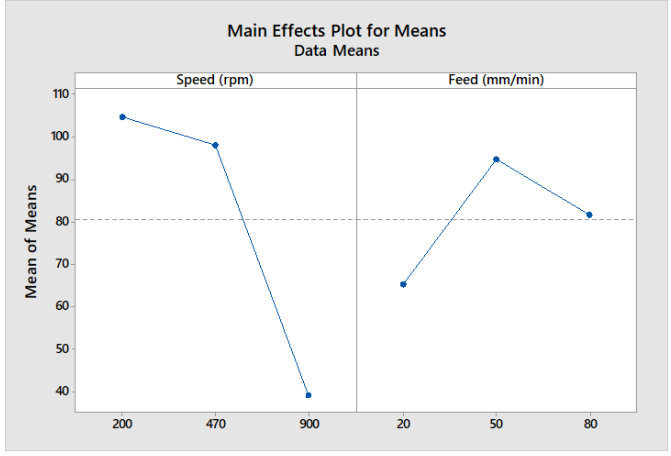

Fig. 20. Main effects plot for feed force, F_y.

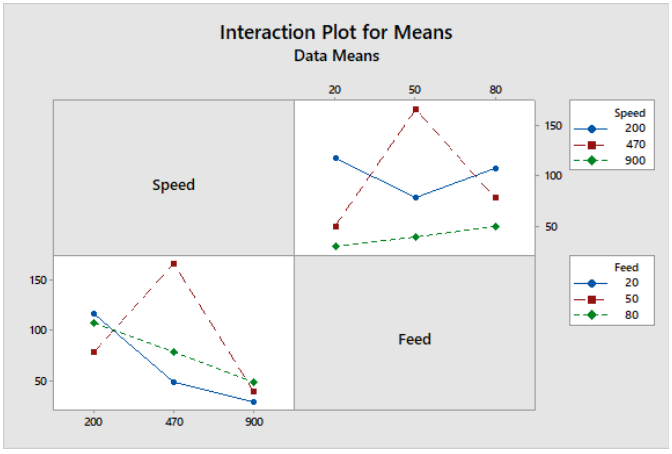

Fig. 21. Interaction plot for Feed Force, F_y.

One-way ANOVA: Fx versus Feed

Method

Null hypothesis	All means are equal
Alternative hypothesis	At least one mean is different
Significance level	α = 0.05

Equal variances were assumed for the analysis.

Factor Information

Factor	Levels	Values
Feed	3	20, 50, 80

Analysis of Variance

Source	DF	Adj SS	Adj MS	F-Value	P-Value
Feed	2	139885	69942	27.48	0.001
Error	6	15269	2545		
Total	8	155154			

Model Summary

S	R-sq	R-sq(adj)	R-sq(pred)
50.4471	90.16%	86.88%	77.86%

Fig. 22. ANOVA table for dominance in cutting force (F_x).

Means

Feed	N	Mean	StDev	95% CI
20	3	294.3	35.4	(223.0, 365.6)
50	3	519.9	68.7	(448.7, 591.2)
80	3	228.9	40.8	(157.6, 300.2)

Pooled StDev = 50.4471

Tukey Pairwise Comparisons

Grouping Information Using the Tukey Method and 95% Confidence

Feed	N	Mean	Grouping
50	3	519.9	A
20	3	294.3	B
80	3	228.9	B

Means that do not share a letter are significantly different.

Fig. 23. Pair-wise results after ANOVA test.

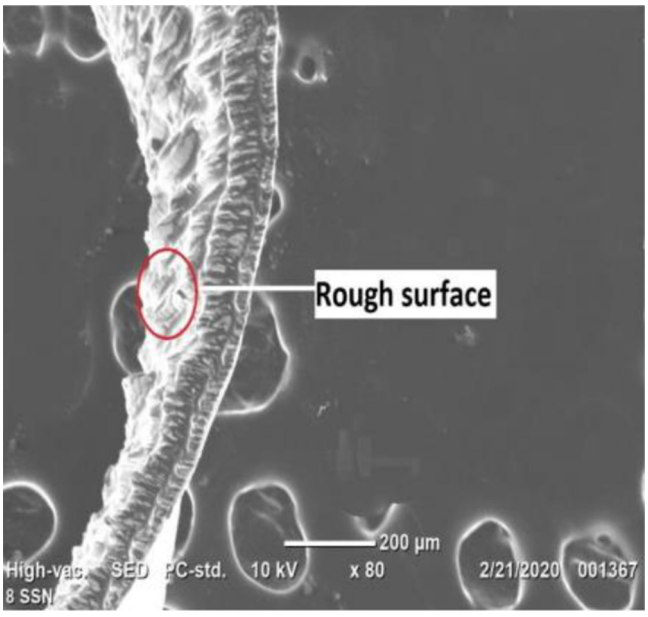

Fig. 24. For cutting speed = 3.77 m/min.

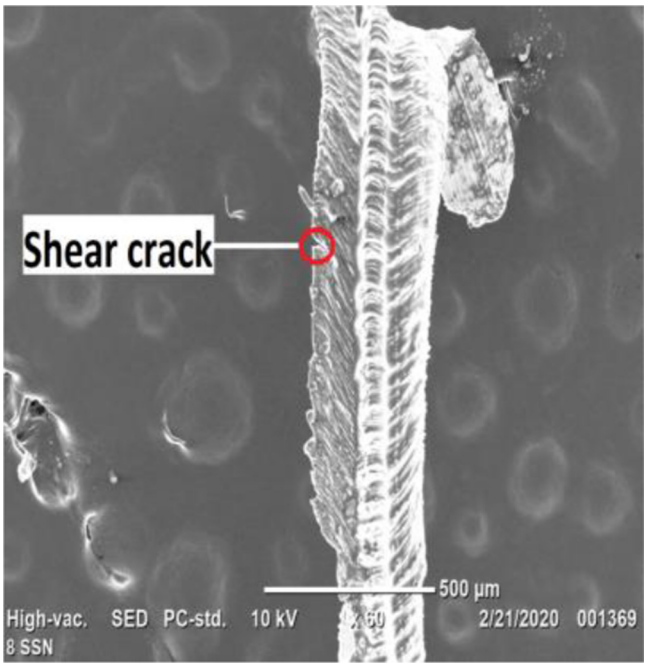

Fig. 25. For cutting speed = 3.77 m/min.

Feed Force (Fig. 21) rather that the other one (Fig. 19). Since Cutting Force (F_x) is a critical response variable, it is pertinent to investigate the statistical significance of influence by its dominant parameter (Feed Rate from DOE Analysis). So ANOVA of Cutting Force (F_x) against Feed Rate becomes appropriate to be conducted. From the ANOVA table (Fig. 22), since p-value (0.001) is less than level of significance ($\alpha = 0.05$) for 95 % confidence, null hypothesis gets rejected. What this means is, statistically significant influence of Feed Rate on Cutting Force, F_x (alternative hypothesis). Further from pair-wise post-ANOVA comparisons by Tukey's method (Fig. 23), it is seen that Medium Feed Rate range influences Cutting Force (F_x) more than other ranges (low and high) grouped together.

For the second phase of work dealing with SEM of machining chips, the results are for four experimental conditions. The first speed (3.77 m/min) shows short chips having tubular, helical shape, a shear crack and generally rough surface with poor finish (Figs. 24 and 25). The shape at this speed may be attributed to shear instability. The second speed (7.54 m/min) results in small, smooth chips with closely-spaced shear bands (Figs. 26 and 27). Thermal softening phenomenon is known to cause shear bands and smoothness of chips indicates optimality of cutting conditions. At the third speed (17.7 m/min), the chips exhibit segmentation and abrasive saw-toothed edges (Figs. 28 and 29). Segmentation is an indication of cross-over of thermal softening boundary to material fracture condition, while saw-toothed edges hint at localized shear, partly owing to machine vibration and chatter. The fourth (33.9 m/min) condition gives rise to chips that are discontinuous, short, helical, serrated and having occasional splits at end (Figs. 30 and 31). Serration is caused by a truncated free surface crack propagation over the chips at intense compressive machining forces.

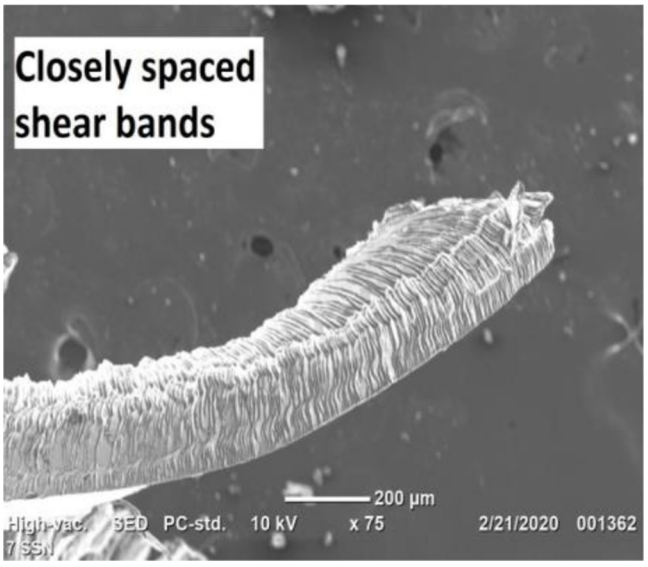

Fig. 26. For cutting speed = 7.54 m/min.

The crux of our work falls in the third phase of FEM simulation. The primary results of interest are Cutting Force (F_x) and Feed Force (F_y). Though any number of secondary results can be obtained using FEA, we restrict ourselves to Tool-Work Interface Temperature alone, as this one has a significant bearing on tool life and stability of process itself. The results provided by the software, Deform 3D, depict primary results of interest (Figs. 32–37, for 3 illustrative selected conditions) as well as secondary (Figs. 38 and 39). One thing to be noted is that FEM can also be used to predict feasibility for imaginary conditions (Figs. 38 and 39). All the parametric settings of

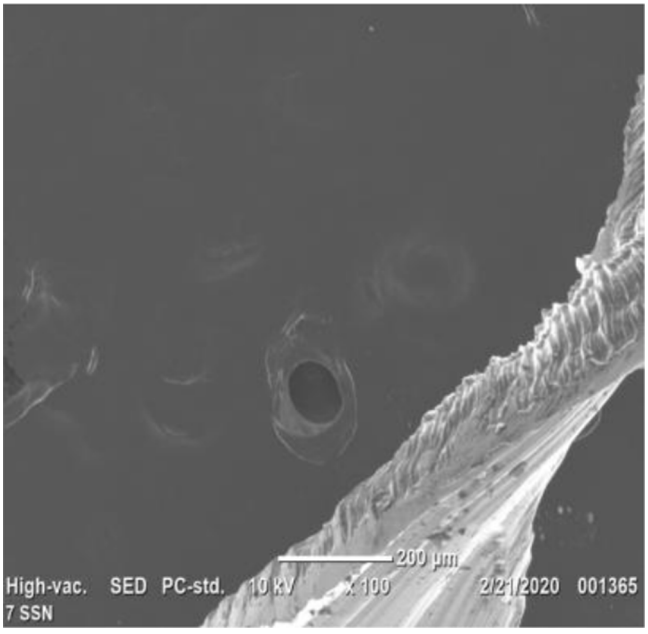

Fig. 27. For cutting speed = 7.54 m/min.

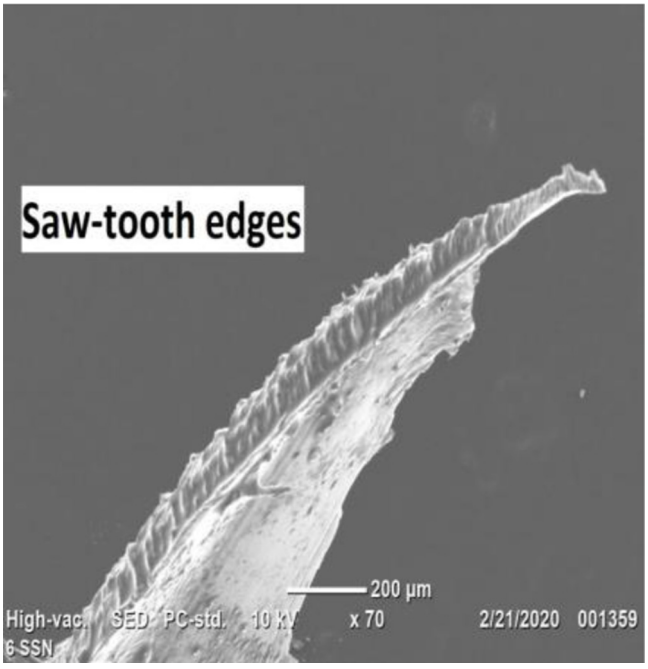

Fig. 28. For cutting speed = 17.7 m/min.

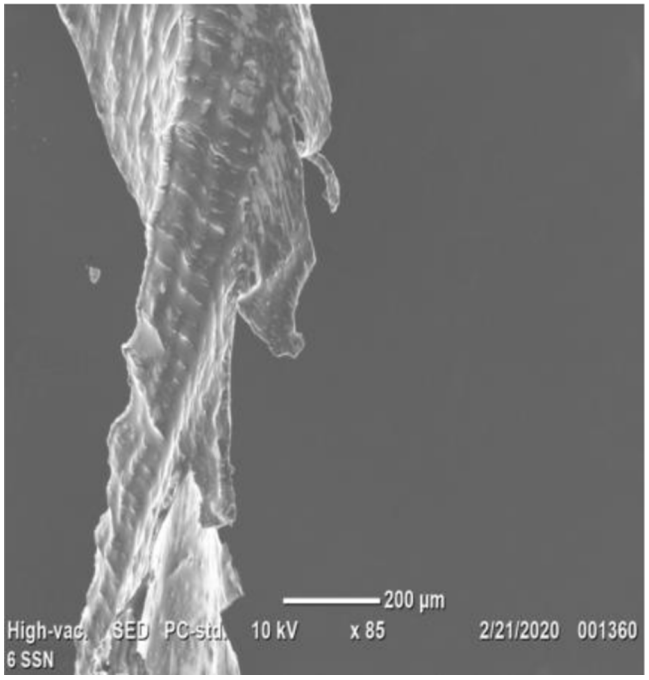

Fig. 29. For cutting speed = 17.7 m/min.

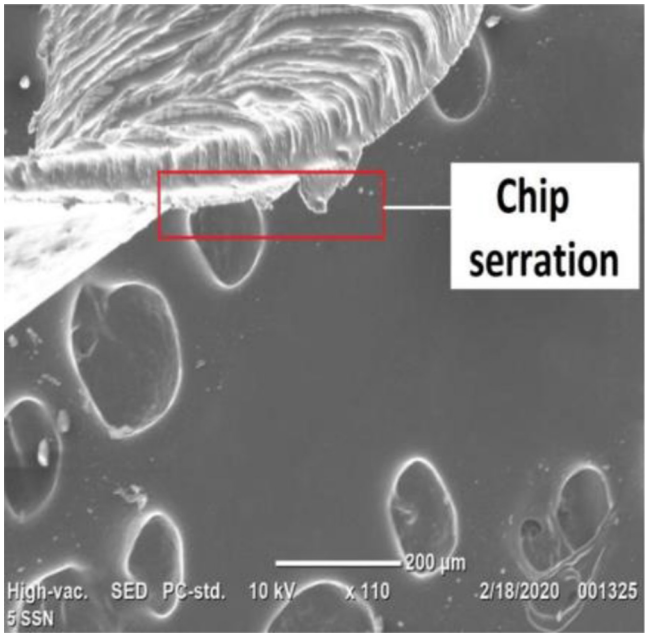

Fig. 30. For cutting speed = 33.9 m/min.

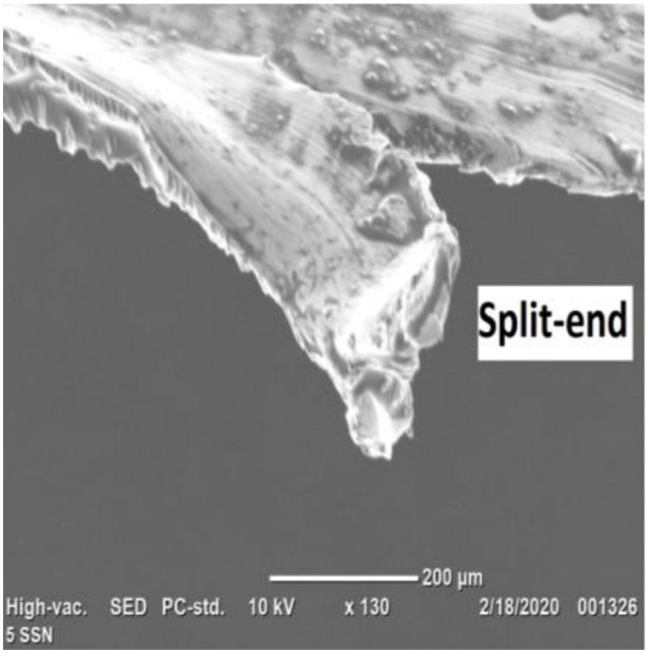

Fig. 31. For Cutting Speed = 33.9 m/min.

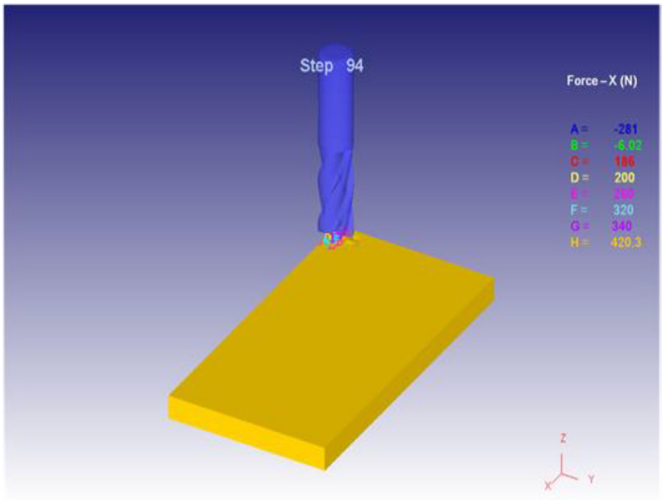

Fig. 32. Mean cutting force, $F_x = 251.67$ N.

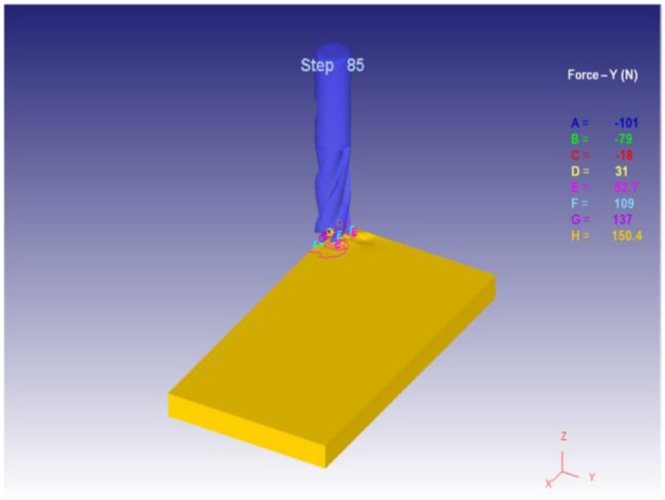

Fig. 33. Mean feed force, $F_y = 84.76$ N. (For Cutting Speed = 7.54 m/min, Feed Rate = 20 mm/min).

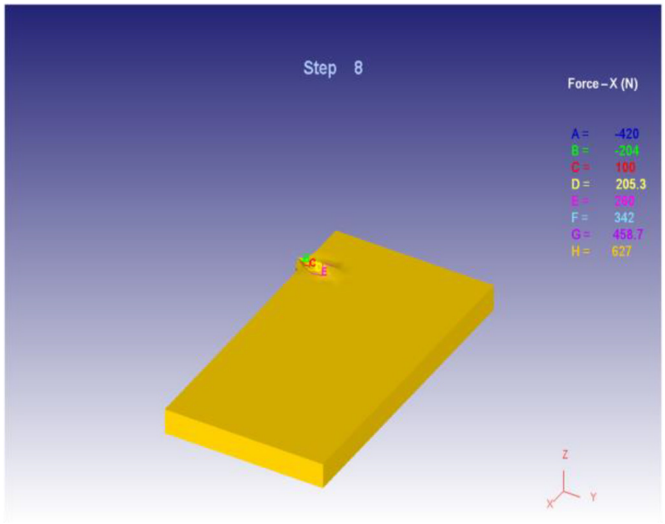

Fig. 34. Mean cutting force, $F_x = 327.13$ N.

the experiment conducted are run in FEM to obtain corresponding results and then tabulated for comparison (Tab. 4). Reasonable convergence is seen here and thus completes the first method of FEM validation. Two other methods are in sequence next.

3.2 Micrographs from SEM for chip morphology

3.2.1 Results from FEA simulation (Deform 3D)

3.2.1.2 Comparison of Stress Values from Software and Extrapolation (FEM Validation – II)

The second FEM validation (Figs. 40 and 41) is by running evaluation of JC Model equation to matching predictive solutions. This verifies that the FEM built is in consonance with the systemic material governing equation. The third final FEM validation is calculative comparison of CDR (Tab. 5), which can vouch for dimensional scale accuracy of FEM formulated. Thus end the three methods of validation of FEM.

4 Conclusions

The following are the conclusions drawn from results of our work:

– Though variation in Cutting Forces throughout the experimental runs appeared to be of random nature, and hence statistically insignificant to establish correlation

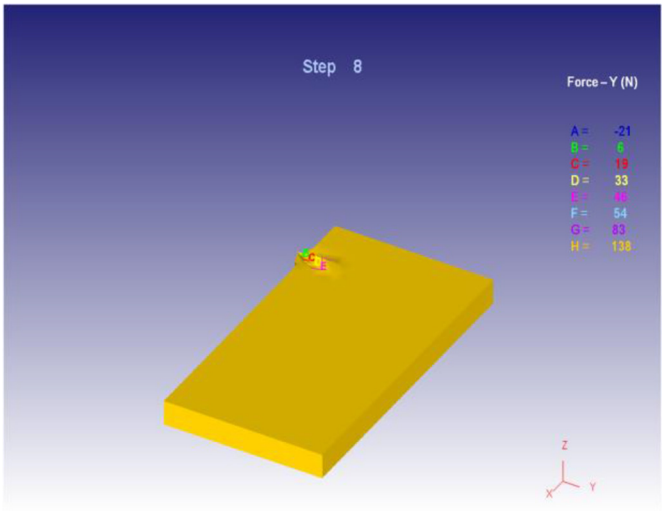

Fig. 35. Mean feed force, $F_y = 50.92\,\text{N}$. (For Cutting Speed = 33.9 m/min, Feed Rate = 20 mm/min).

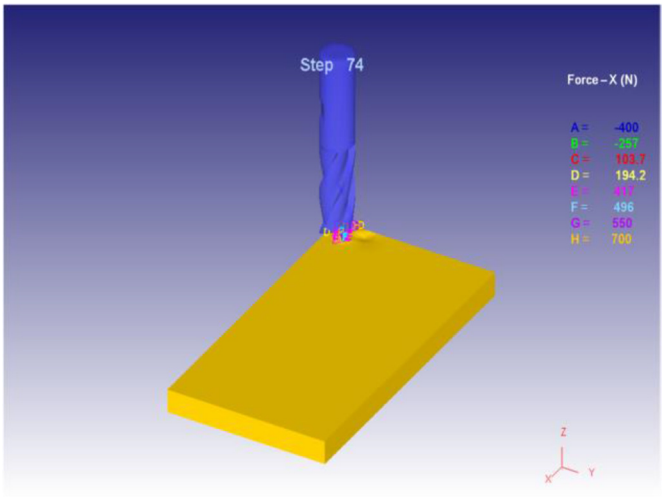

Fig. 36. Mean cutting force, $F_x = 504.23\,\text{N}$.

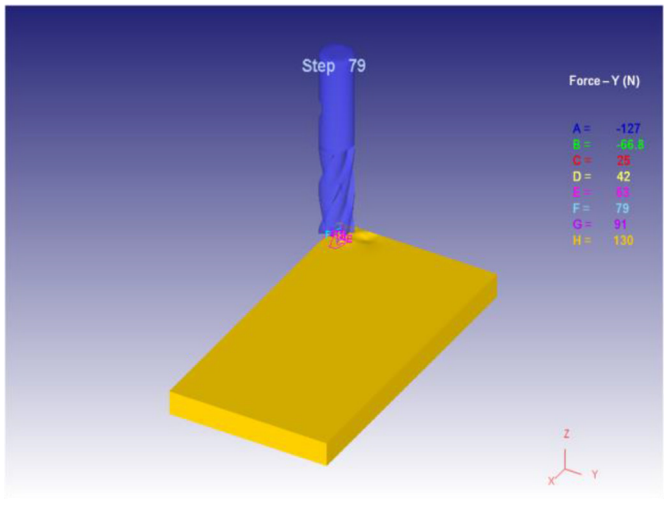

Fig. 37. Mean feed force, $F_y = 42.56\,\text{N}$. (For Cutting Speed = 33.9 m/min, Feed Rate = 50 mm/min).

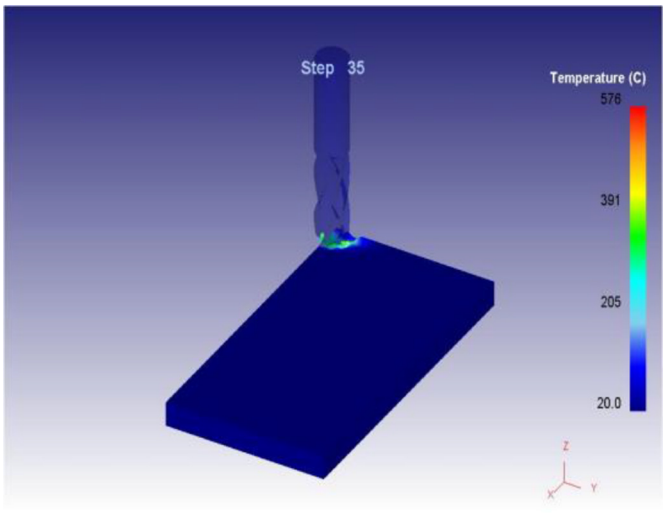

Fig. 38. Tool-work interface temperature = 849 K.

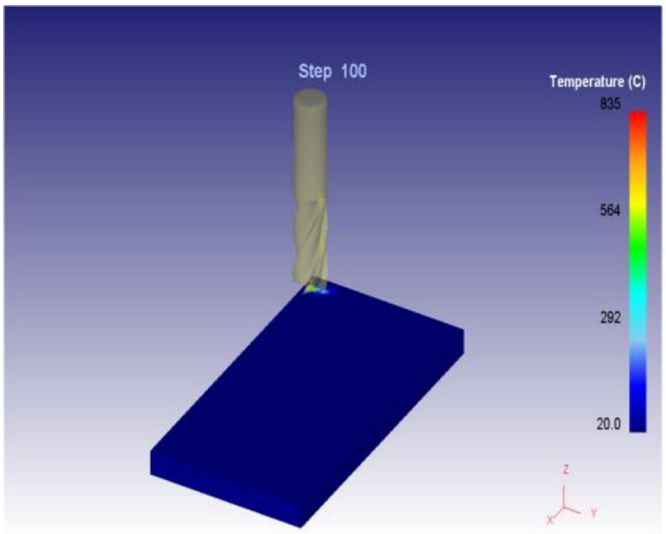

Fig. 39. Tool-work interface temperature = 1108 K. (For conditions at 303 K ambience, 1. Feed Rate = 35 mm/min, Rotational Speed = 300 rpm & 2. Feed Rate = 75 mm/min, Rotational Speed = 700 rpm, in respective order).

by ANOVA, Feed Rate is seen to significantly influence Cutting Force, as revealed by DOE Analysis results. Further by graphical plots, we concur that High Feed Rates are not at all advisable for the end-milling process of Inconel 718.

– Exhaustive investigation into the cutting process of end-milling, by way of chip morphology studies using SEM images of machining chips from experiment, made us realize that medium Cutting Speeds appear favorable to milling of Inconel 718. This is because on the lower end of the Cutting Speed spectrum, there is possibility for a rough surface finish, while on the higher end, chip serrations, split and saw tooth faced chip edges may impede efficient end-milling.

Table 4. Comparison of force values from software and experiment (FEM validation − I).

Cutting speed (m/min)	Feed rate (mm/min)	Cutting force, F_x (N)		Feed force, F_y (N)		Error [%]	
		Experimental	FEA	Experimental	FEA	Cutting force, F_x	Feed force, F_y
7.54	20	333.54	251.67	117.72	84.76	24.55	28.00
7.54	50	598.41	644.42	78.48	92.53	7.69	17.90
7.54	80	147.15	202.95	117.72	134.24	37.92	14.03
17.7	20	284.49	389.75	49.05	77.98	37.00	58.98
17.7	50	470.88	493.15	166.77	220.5	4.73	32.22
17.7	80	215.82	198.62	78.48	40.21	7.97	48.76
33.9	20	264.87	327.13	58.86	50.92	23.51	13.49
33.9	50	490.50	504.23	39.24	42.56	2.80	8.46
33.9	80	274.68	267.98	49.05	56.40	2.44	14.98

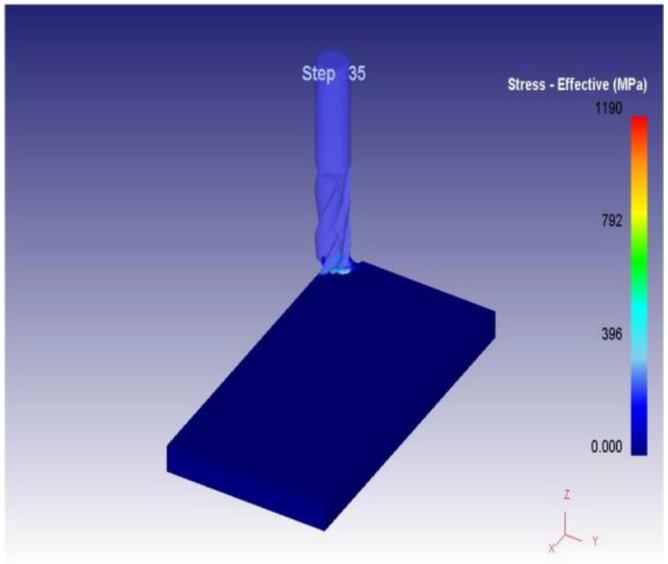

Fig. 40. Von-Mises Stress = 1190 Mpa.

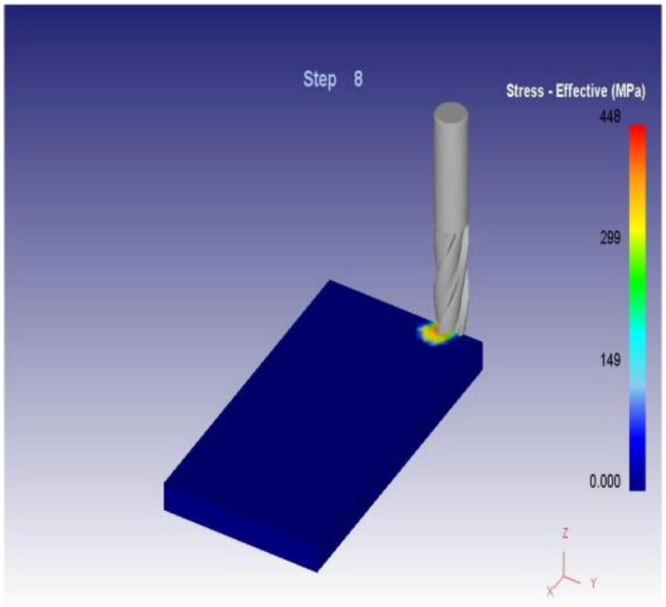

Fig. 41. Von-Mises Stress = 448 Mpa. (For conditions at 303 K ambience, 1. Feed Rate = 35 mm/min, Rotational Speed = 300 rpm, JC Model gives 1193.38 MPa & 2. Feed Rate = 75 mm/min, Rotational Speed = 700 rpm, JC Model gives 439.28 MPa; in respective order).

Table 5. Comparison of CDR from software and experiment (FEM Validation − III).

Machining Condition (Cutting Speed) [m/min]	Mean Value of Experimental Chip Dimension (mm)	Corresponding Chip Dimension from FEA Simulation (mm)	Calculated CDR		
			By Experiment	From FEA Simulation	Error [%]
33.9	0.814	0.780631	1.628	1.561	4.11
17.7	0.7395	0.730666	1.479	1.461	1.21
7.54	0.9005	0.847187	1.801	1.694	5.94
3.77	0.9075	0.849835	1.815	1.699	6.39

– Successful computer simulation of the end-milling process based on FEA was undertaken, using a suitable software (Deform 3D) followed by sufficient validation of the FEM created by various methods. Good agreement of Forces in Milling between experiment and FEA, consonance of Flow Stress values obtained by predictive modeling with JC Model parametric extrapolation and additional verification by means of CDR stand testimony to the very fact.
– Optimum experimental conditions of end-milling of Inconel 718, from our overall work are seen to be within the ranges: 20–50 mm/min for Feed Rate and 200–500 rpm for Spindle (Cutting) Speed.

5 Implications and influences

With the ability to simulate on a computer a machining process like end-milling for a critical material (like Inconel 718 or others), and thence also get an idea of the most important determiner of process stability (Cutting Force) as a function of plausible machining parameters (Cutting Speed and Feed Rate), a machinist or manufacturing engineer will be in a better position to leverage optimized experimental conditions. This can in turn, improve overall production output metrics and process efficiency, with a positive spill-over to the entire production line. As to the future scope of study, it may be commented that choice of material for the cutting tool, examination of F_z component (or Depth of Cut) as an additional variable, effect of increased number of machining passes, simulation on other popular FEA tools and newer methods of their validation are some directive clues that may be looked into for extension and augmentation upon the current work.

References

1. K. Venkata Rao, B. Bachina Harish Babu, V. Umasai Vara Prasad, A study on effect of dead metal zone on tool vibration, cutting and thrust forces in micro milling of Inconel 718, Alloys Compd. 793 (2019)
2. M. Rahman, W.K.H. Seah, T.T. Teo, The Machinability of Inconel 718, Mater. Process. Technol. **204**, 63–199 (1997)
3. R. Merugu, S. Datta, Effects of Cutting Speed on Chip Characteristics and Tool Wear Mechanisms During Dry Machining of Inconel 718 Using Uncoated WC Tool, Arab. J. Sci. Eng. **44**, 7423–7440 (2019)
4. U. Necati, A. Cicek, K. Aslantas, Proceedings of the 17th CIRP Conference on Modeling of Machining Operations, Finite Element Simulations of cutting force, torque, and temperature in drilling of Inconel 718 (2019)
5. M. Alauddin, M.A. Mazid, M.A. El Baradi, M.S.J. Hashmi, Cutting Forces in the end milling of Inconel 718, Mater. Process. Technol. **77**, 153–159 (1998)
6. D. Thakur, B. Ramamoorthy, L. Vijayaraghavan, Optimization of high speed turning parameters of super-alloy Inconel 718 material using Taguchi technique, Indian J. Eng. Mater. Sci. **16**, 44–50 (2008)
7. J. Lorentzona, N. Jarvstrat, B.L. Josefson, Modeling chip formation of alloy 718, J. Mater. Process. Technol. **209**, 4645–4653 (2009)
8. K.S. Vijay Sekar, P.R. Shivaram, K. Sushinder, S.B. Nivedh Kannaa, N. Gupta, Experimental Investigation and Finite Element Analysis of milling of Ti-6Al-4V Titanium alloy by studying cutting forces and chip microstructure, Appl. Mech. Mater. 852 (2016)
9. A. Del Pretea, L. Filice, D. Umbrello, Proceedings of the 14th CIRP Conference on Modeling of Machining Operations [CIRP CMMO], Numerical Simulation of Machining Nickel-Based Alloys (2013)
10. P. Angelos, Markopoulos, in Finite Element Method in Machining Processes, Springer- ISBN 978-1-4471-4330-7

Cite this article as: Akhil C. Kuriakose, Raman Balakrishnan, Harsh Vardhan, Krishnaraju Srinivasaraju Vijay Sekar, Experimental investigations and finite element analysis of milling of Inconel 718 alloy, Int. J. Simul. Multidisci. Des. Optim. **12**, 21 (2021)